

Semi-Parametric Color Reproduction Method for Optical See-Through Head-Mounted Displays

Yuta Itoh, *Student Member, IEEE*, Maksym Dzitsiuk, Toshiyuki Amano, *Member, IEEE*, and Gudrun Klinker, *Member, IEEE*



Fig. 1. A demonstration of the color reproduction problem in OST-HMDs and a result of our correction method. (a) A physical scene captured by a user-perspective camera. (b) A captured image of (a) rendered on a consumer OST-HMD with an opaque background. (c) A captured image of a pre-processed image of (a) displayed on the HMD. Rendering (a) on the display causes chromatically distorted image (b), which is undesirable for natural AR experiences. The corrected image (c) reproduces the original color better, thus potentially provides better color constancy in visual-processing AR applications.

Abstract— The fundamental issues in Augmented Reality (AR) are on how to naturally mediate the reality with virtual content as seen by users. In AR applications with Optical See-Through Head-Mounted Displays (OST-HMD), the issues often raise the problem of rendering color on the OST-HMD consistently to input colors. However, due to various display constraints and eye properties, it is still a challenging task to indistinguishably reproduce the colors on OST-HMDs. An approach to solve this problem is to pre-process the input color so that a user perceives the output color on the display to be the same as the input.

We propose a color calibration method for OST-HMDs. We start from modeling the physical optics in the rendering and perception process between the HMD and the eye. We treat the color distortion as a semi-parametric model which separates the non-linear color distortion and the linear color shift. We demonstrate that calibrated images regain their original appearance on two OST-HMD setups with both synthetic and real datasets. Furthermore, we analyze the limitations of the proposed method and remaining problems of the color reproduction in OST-HMDs. We then discuss how to realize more practical color reproduction methods for future HMD-eye system.

Index Terms— OST-HMD, color replication, color calibration, optical see-through display.

1 INTRODUCTION

One of the most fundamental issues in Augmented Reality (AR) is how to mediate virtual contents and physical scenes consistently so that the contents appear as realistic as possible. In AR applications with an Optical See-Through Head-Mounted Display (OST-HMD), the display imposes virtual contents into a user’s field of view (FoV) directly. Since the user perceives the contents together with the physical world as a reference in which the contents are registered, the user will immediately exclude the virtual contents if their appearance is implausible compared to the observed reality in the same view.

We believe that a future, ultimate OST-HMD is capable of provid-

ing users with visual stimuli that are indistinguishable from the reality. However, current OST-HMDs can not realize such truly natural AR experiences due to various reasons. The key question is how to render virtual contents consistently with reality. In other words, an OST-HMD has to present visual information adapted seamlessly to the reality in various aspects: temporally, spatially, and visually. Among them, the visual consistency is the focus of this paper.

In AR applications, a visually-consistent OST-HMD system must create visual stimuli as exactly as specified: if we input a digital RGB color, the display should reproduce a color which an eye perceives as the same color (Fig. 1). This truthful color reproduction is a fundamental requirement for any OST-HMD system so that they can further benefit from related visual processing techniques in AR, e.g. rendering with global illumination [1], appearance control of physical objects [2, 3], and vision enhancement [4].

In current HMDs, this is not the case. For example, if a system tries to render a virtual, white spotlight on a real object while the display has bluish color distortion, then the virtual light appears bluish instead of pure white *even if* the system takes the scene illumination and the radiometric property of the object into account. This is analogous to the spatial registration between an OST-HMD and the real world: even if the 3D structure of the world is perfectly known, virtual contents still appear misaligned if the calibration between an OST-HMD and a user’s eye position is inaccurate.

Note that the semitransparent medium of an OST-HMD also causes

- Yuta Itoh is with the Department of Informatics at Technical University of Munich. E-mail: itoh@in.tum.de
- Maksym Dzitsiuk is with the Department of Informatics at Technical University of Munich. E-mail: max.dzitsiuk@tum.de
- Toshiyuki Amano is with the Faculty of Systems Engineering at Wakayama University. E-mail: amano@sys.wakayama-u.ac.jp
- Gudrun Klinker is with the Department of Informatics at Technical University of Munich. E-mail: klinker@in.tum.de

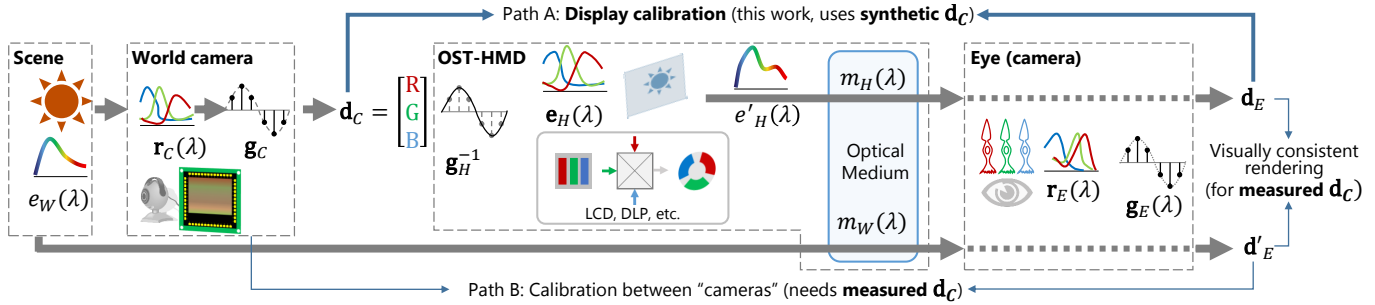


Fig. 2. An overview of color calibration problems on an OST-HMD system. Our display calibration problem is to calibrate the HMD and the eye camera (Path A). In this case \mathbf{d}_c is synthetic color. As introduced in the evaluation section, a scene image taken by a world camera is needed to measure visual consistency of AR rendering (Path B and the text on the right of the diagram). In this case \mathbf{d}_c is physically measured color.

a color blending problem between the background scene and a displayed image. However, this paper does not focus on this issue which can be solved by introducing an opaque layer in the display design [5, 6]. Once the display color is correctly calibrated, the blending problem can be solved by subtracting a measured background color from a target color to be rendered [7].

The other causes of the color discrepancy in OST-HMDs are mainly twofold: light absorption by the imperfect optical medium of the HMD and lossy digital-analog color conversion between the HMD and an eye.

OST-HMDs have complex optics that propagates a virtual image from the display image source to a user’s eye by refracting the light typically via beam-splitting mirrors or free-form prisms [8, 9] (Path A in Fig. 2). Since the user sees the virtual image through these semi-transparent optical media, the spectrum of the light that reaches to the user’s eye is not necessarily identical to the original one emitted from the image source [10].

The rendering/perception process of the HMD-eye system, i.e the color transfer from the light source of the HMD to the photoreceptors of a human eye, causes another color distortion. When the HMD renders a digital color \mathbf{d}_c , the display emits the data as a physical light with analog spectrum. The light is then re-converted to *color data* by the photoreceptors of an eye (and our brain) which has a different spectral response than that of the image sensor. Since these analog-digital color conversions inevitably lose information, just rendering a target color on the HMD can not reproduce the same color at the eye.

These two reasons combined, estimating color distortions in OST-HMDs becomes a challenging task. A naive way is to create a look-up table (LUT) between the input and the actually perceived color. While the calibration based on this approach is simple, it is costly in memory size and does not consider any prior knowledge, i.e. physical phenomena of the display system. Incorporating a physical model would give us room to extend the calibration model by updating it in the future.

We focus on the color reproduction problem while featuring the color processing flow in HMD-eye systems (Path A in Fig. 2). We propose a semi-parametric color calibration method that makes use of the knowledge from projector-camera systems (PCS) and ordinary display calibration techniques. We learn the color response between a user-perspective camera (a camera located at the eyepoint to acquire data and calibrate) and each color channel of the display.

A display in general has a non-linear relationship between the input digital color and the produced light intensity. This relationship is typically observed as a smooth curve called the gamma curve. Our method learns a color mapping function as the combination of the correction of this gamma curve and a linear conversion of color channels with a post-scaling adjustment. More importantly, we provide a thorough analysis of the current color reproduction setup including limitations, research issues, and possible solutions for indistinguishable color visualization in OST-HMD systems.

Contributions

Our main contributions are the following:

- We propose a semi-parametric color calibration method which incorporates the optical properties of OST-HMD systems
- We provide a thorough evaluation of the proposed method including limitations and discussions for more practical color reproduction in HMD-eye system.

We also state a general color reproduction problem in OST-HMDs on top of color models in PCS and display calibration fields.

2 RELATED WORK

As the HMD-eye system is analogous to the PCS, this section elaborate these problems along works of PCS. We first introduce visual-processing AR applications that are potentially transferable to OST-HMD systems; yet need an accurate color reproduction to do so. We then overview color calibration research in display systems including PCSs and OST-HMDs.

2.1 Visual Consistency in AR Applications

In video-based AR, various works aim to enhance the realism of AR rendering. Their methods implicitly stand on accurate color reproduction of a display, which is rather easy to achieve on video-based systems by integrating virtual contents directly into captured images. Lee and Woo [11] propose a method which reflects the illumination of a scene into the rendering of virtual objects by referring to the reflection on a fiducial marker. Knorr and Kurz [12] estimate a scene illumination from the reflection of light on human faces, and realize coherent AR visualization with the estimated illumination. Fischer et al. [13] incorporate the sensor noise and the motion blur of a camera when rendering virtual objects by blurring and adding synthetic noise on an output image.

In spatial AR, various systems target on augmenting the appearance of physical objects. Menk and Koch [14] present a visualization system which reproduces desired input color on a physical, miniature 3D car model by a PCS. Amano and Kato [2] propose a dynamic PCS system which controls the appearance of scene objects via dynamic camera projector feedback.

If we want to transfer these visual-processing techniques to OST-HMD systems, assuring the color reproducibility will be a critical issue. Our recent work on a vision enhancement for defocus correction with OST-HMDs [4] is also an example that requires perfect color reproduction between the scene and a displayed enhancement image. The next section elaborates works related to the color constancy in display systems including the OST-HMDs.

2.2 Color Reproduction in Display Systems

Since the popularization of projectors, printers and digital cameras, researchers have tackled the topic of calibrating colors for such image media [15, 16, 17, 18, 19, 20, 21, 22]. The OST-HMD technology, however, still lacks elaborate study on color reproduction. Since this problem on OST-HMDs is significantly cross-correlated with that for

other types of displays – especially PCS, we survey existing color reproduction methods in the related display technologies.

We can see a general color reproduction problem as the following: given a target color \mathbf{d}_E perceived by an eye E , and some prior knowledge θ of the display and the environment, we want to find an input color for the display as $\mathbf{d}_C = f(\mathbf{d}_E, \theta)$, where f conceptually represents the inverse of image rendering process from a display to the image \mathbf{d}_E perceived by the eye (or a camera).

Intuitively speaking, f is a color mapping between two images. Note that \mathbf{d}_C and \mathbf{d}_E may have some constraints due to their sensors such as dynamic range limitation. Depending on how we define f , existing methods can be classified into a non-parametric, a parametric, and a semi-parametric approaches.

2.2.1 Non-Parametric Approach

In non-parametric methods, f is locally defined by each target color value \mathbf{d}_E . The *most* non-parametric approach is to use LUTs [20, 14, 23, 10, 18]. LUT-based methods are purely non-parametric since each target color \mathbf{d}_E is mapped to the corresponding input color \mathbf{d}_C independently. In general, these methods are not suitable for direct color mapping: unlike with projectors and printers, OST-HMDs are often based on mobile processors and graphic chips. Such systems thus can not perform huge number of transformations with an acceptable frame rate when traversing big LUTs (see Sec. 3 for a LUT size estimate). Since the LUT method uses pixel-to-pixel correspondences, it is prone to noise.

Hincapié-Ramos et al. [10] propose an LUT-based approach for projectors that is further developed to be applicable for color correction on OST-HMDs at run-time [23]. This method suggests splitting the entire CIE Lab color space into bins of similar colors which is followed by building a LUT between target and displayed colors. The later work also proposes an optimization for a search in the LUT and implementation of the algorithm as a GPU shader program that can be used in real time.

Note that the above methods do not incorporate prior knowledge θ . Our work is targeted at the same problem, but with a different approach which is derived from the physical model of the process.

Porikli [21] presents an inter-camera color correction method, which learns a LUT based on the correlation between training color samples $\{\mathbf{d}_C\}$ taken by a source camera and $\{\mathbf{d}_E\}$ taken by a target camera, and the method aims to learn the change of sensor responses between both cameras. Kagarlitsky et al. [24] extend the correlation approach by incorporating image segmentation to apply the mapping for local image regions that possibly have different lighting conditions.

2.2.2 Parametric Approach

In parametric methods, f is defined within a set of functions that can be parametrized by some variables. Our eyes or cameras perceive color by trichromatic photoreceptors or sensors. Displays normally take 3D RGB input values. Therefore, f is often modeled as a 3-by-3 matrix M , and the problem becomes how to estimate this linear mapping between \mathbf{d}_C and \mathbf{d}_E .

A well-known model is the von-Kries adaptation [25], also called diagonal correction [26], where each color channel intensity value is linearly scaled by a multiplicative factor. This does not hold for OST-HMDs as well because of the assumption of the linear color response [19]. In Sec. 5 we reconfirm empirically that commercial OST-HMDs also have this non-linear response to be corrected.

Reinhard et al. [27] determine M by performing a histogram match to transfer colors from one image $\{\mathbf{d}_C\}$ to another $\{\mathbf{d}_E\}$. This approach is purely image-oriented and does not consider the physical model of displays. Their method does not consider the gamma since the effects is often negligible in their inter-image color correction setup.

2.2.3 Semi-Parametric Approach

The nuisance of the color reproduction on displays is that the rendering process induces various non-linear effects such as the gamma curve. These non-linear effects are hard to handle with simple parametric functions while they are computationally efficient. Although

the non-parametric approach is capable of handling the non-linearity, it can be computationally expensive and can require a huge memory space.

To get benefits from both methods, one can consider combining a non-parametric and a parametric function. A common way is to first correct the gamma curve of the projector response. Nayar et al. [28] propose a color correction method for PCSs by modeling the imaging process of PCSs as the combination of a linear, color-mixing matrix and non-linear radiometric responses per color channel. Menk and Koch [14] also propose a similar method by modeling the distortion as the combination of 1D intensity gamma distortion and 3-by-3 color conversion matrix, in addition to the scene illumination θ as a function of the camera position.

In this work, we follow a semi-parametric approach. We aim to model the color distortion following the actual optical rendering process of OST-HMDs similar to [28]. Our calibration procedure examines the color response of each color channel of the image source of an OST-HMD, and then estimate the linear parameters and non-linear functions of the model.

3 METHOD

For OST-HMDs, virtual objects are presented next to physical objects existing both within the FoV of the HMD and outside of it (in the peripheral viewing range of the user). For these displays, it is critical that added virtual objects blend perfectly into such physical environment.

To test such situations, it is not enough to merely display and evaluate the color properties of synthetic virtual objects (Path A in Fig 2). They need to be seen in physical context.

A practical approach for such comparison is to generate virtual object data via photographs of the physical world (by a *world* camera) and to compare the displayed colors of such an image (as seen by a user-perspective camera) with the original color image itself (the right text in Fig 2).

In other words, the goal of the color calibration can be separated into two problems: calibration between an OST-HMD and an eye (\mathbf{d}_C and \mathbf{d}_E , Path A), and between a world-looking camera and an eye *camera* (\mathbf{d}_C and \mathbf{d}'_E , Path B).

This paper focuses only on the former problem (Path A). The latter can be tackled independently from the former. Our evaluation also compares \mathbf{d}_E and \mathbf{d}'_E with a physically measured \mathbf{d}_C to see the potential performance of our calibration for AR rendering setups. For this, as we later explain, our exemplifying setup assumes that the Path B is negligible since we use a single camera as the world and eye camera.

In the following, we first model a general color rendering process of the HMD-eye system, then we introduce our calibration approach.

3.1 Notations

Ordinary lower-case letters denote functions and scalar values such as a radiometric response function $e(\lambda)$ with the scalar wavelength λ . Bold lower-case letters denote multi-valued functions and vectors such as an RGB sensor response function $\mathbf{r}(\lambda)$ and an RGB color triplet \mathbf{d} . Upper typewriter letters denote matrices such as M . We use $(\cdot)^T$ for the transpose of vectors and matrices, $(\cdot)^{-1}$ for the inverse of functions/matrices, and \circ for the element-wise product of arrays. Upper-case black-bold letters denote sets such as the set of non-negative real numbers $\mathbb{R}_{\geq 0}$ and of integers \mathbb{N} . We assume digital colors ranged from 0 to 255 and denote the integer set as $\mathbb{N}_{[0,255]}$.

3.2 Radiometric Model of OST-HMDs

We first introduce a general radiometric model of an OST-HMD setup. Later in the next section, we derive a simplistic model out of the general model so that we can for now handle with our OST-HMD setup. For a more practical calibration, we cannot avoid working on the general model, which is still a challenging task with existing HMD technologies. Note that the radiometric model of OST-HMDs has a close relationship to that of PCSs.

3.2.1 Display-eye calibration | Path A in Fig. 2

Given an input digital color $\mathbf{d}_c \in \mathbb{N}_{[0,255]}^3$, the display produces a three-dimensional spectral distribution as a function of a wavelength:

$$\mathbf{e}_H(\lambda | \mathbf{d}_c) \in \mathbb{R}_{\geq 0}^3, \quad (1)$$

where each element of \mathbf{e}_H corresponds to each RGB filter of the display light source. We assume that each element of the function is independent from its channel brightness:

$$\mathbf{e}_H(\lambda | \mathbf{d}_c) = \mathbf{g}_H^{-1}(\mathbf{d}_c) \circ \mathbf{e}_H(\lambda), \quad (2)$$

where $\mathbf{g}_H^{-1}(\cdot) : \mathbb{N}_{[0,255]}^3 \rightarrow \mathbb{R}_{\geq 0}^3$ is the brightness of the display which modulates the base spectral distribution of the display: $\mathbf{e}_H(\cdot) : \mathbb{R}_{\geq 0} \rightarrow \mathbb{R}_{\geq 0}^3$. Under this model, the display emits the following light:

$$e'_H(\lambda) := \sum_{k=1}^3 [\mathbf{e}_H(\lambda | \mathbf{d}_c)]_k = \mathbf{g}_H^{-1}(\mathbf{d}_c)^T \mathbf{e}_H(\lambda) \in \mathbb{R}_{\geq 0}. \quad (3)$$

The eye perceives the display light $e'_H(\lambda)$. Although modeling human color vision is yet another challenging topic, let us for now consider a user perspective camera E as a replacement of an eye. Let $\mathbf{g}_E(\cdot) : \mathbb{R}^3 \rightarrow \mathbb{N}_{[0,255]}^3$ be the gamma function of the camera. Then the camera outputs

$$\mathbf{d}_E := \mathbf{g}_E \left(\int e'_H(\lambda) m_H(\lambda) \mathbf{r}_E(\lambda) d\lambda \right) \quad (4)$$

$$= \mathbf{g}_E \left(\int \left(\mathbf{g}_H^{-1}(\mathbf{d}_c)^T \mathbf{e}_H(\lambda) \right) m_H(\lambda) \mathbf{r}_E(\lambda) d\lambda \right), \quad (5)$$

where $m_H(\lambda)$ represents an intensity loss of the light when it propagates a light path from the image source to the camera sensor through the medium, and $\mathbf{r}_E(\lambda)$ is an efficiency function of the camera sensor.

Note that the digital color vector \mathbf{d}_c is the only parameter we can control as an input of Eq. (3). A naive way to find the best \mathbf{d}_c is a brute force approach where we display all possible color combinations of \mathbf{d}_c and measure resulting \mathbf{d}_E . Then we create a huge look-up table from \mathbf{d}_E to \mathbf{d}_c . This non-parametric, discrete approach requires extra memory and calibration time. For example, if we use 8-bit RGB color model, the table size becomes about 50MB ($\approx 256^3 * 8 * 3$ bit) and recording all color responses would take more than 6 days even if we can capture each color in 30Hz non-stop.

Hincapié-Ramos et al. [23] extended this approach and proposed a real-time method by binning the table entries in a CIE Lab color space to compress the overall table size while keeping the matching quality reasonable. Unlike these pure non-parametric approaches, we further investigate the physical model of OST-HMDs to derive a simpler model. We believe modeling the system based on its physical mechanism leaves us more room to improve the model in the future.

Since $\mathbf{g}_H^{-1}(\mathbf{d}_c)$ is independent from λ , we reformulate Eq. (5) as

$$\mathbf{d}_E = \mathbf{g}_E \left(\underbrace{\int \left(m_H(\lambda) \mathbf{r}_E(\lambda) \mathbf{e}_H(\lambda)^T \right) d\lambda}_{=: \mathbf{M}} \mathbf{g}_H^{-1}(\mathbf{d}_c) \right) = \mathbf{g}_E(\mathbf{M} \mathbf{g}_H^{-1}(\mathbf{d}_c)), \quad (6)$$

where $\mathbf{M} \in \mathbb{R}^{3 \times 3}$ is a constant, color conversion matrix. The color distortion is now modeled as a semi-parametric model which consists of two non-linear functions $\{\mathbf{g}_E, \mathbf{g}_H^{-1}\}$ and the linear matrix.

We employ the following relationship between the target color \mathbf{d}_E and the input color \mathbf{d}_c ,

$$\mathbf{d}_E = \mathbf{g}_E(\mathbf{M} \mathbf{g}_H^{-1}(\mathbf{d}_c)), \quad (7)$$

$$\mathbf{d}_c = \mathbf{g}_H(\mathbf{M}^{-1} \mathbf{g}_E^{-1}(\mathbf{d}_E)). \quad (8)$$

Our problem is now how to estimate \mathbf{g}_H , \mathbf{M}^{-1} , and \mathbf{g}_E^{-1} from training data $(\mathbf{d}_c, \mathbf{d}_E)$. Before explaining this, we briefly introduce the concept of visually consistent AR rendering in the next section.

3.2.2 Visually consistent AR rendering | Fig. 2 Path B and right

In AR applications with OST-HMDs, a user sees the physical world and virtual image in the same FoV. If the light from the world and that from the display coincide, then an observer can not distinguish, in terms of color, if a perceived color is from the display or directly from the world. However, this is unlikely to occur in practice – the image sensor of a camera and the photoreceptors of an eye have different responses, thus the image source of an HMD can not reproduce the original light spectra by mere, typically, three RGB light channels.

Fortunately, our cone cells (and image sensors) cannot distinguish light with different spectra if they cause the equivalent amount of electrical charge in the cells – the phenomena which is known as metamerism, thus we consider perceived color spaces.

Consider a camera C placed in the world W (Fig. 2 Path B). The camera captures light from the world with a spectral distribution $e_w(\cdot) : \mathbb{R}_{\geq 0} \rightarrow \mathbb{R}_{\geq 0}$, then converts the light into an RGB vector:

$$\mathbf{d}_c := \mathbf{g}_c \left(\int e_w(\lambda) \mathbf{r}_c(\lambda) d\lambda \right) \in \mathbb{N}_{[0,255]}^3, \quad (9)$$

where $\mathbf{r}_c(\cdot) : \mathbb{R}_{\geq 0} \rightarrow \mathbb{R}_{\geq 0}^3$ is an efficiency function of the camera sensor and $\mathbf{g}_c(\cdot) : \mathbb{R}^3 \rightarrow \mathbb{N}_{[0,255]}^3$ is a sensor gamma function which converts analog signals to digital values.

The eye camera sees the color of the real world as:

$$\mathbf{d}'_E := \mathbf{g}_E \left(\int e_w(\lambda) m_w(\lambda) \mathbf{r}_E(\lambda) d\lambda \right), \quad (10)$$

$m_w(\lambda)$ represents an intensity loss due to the medium of the OST-HMD. Note that $m_w(\lambda)$ is not necessarily same as $m_H(\lambda)$.

Overall, visually consistent AR rendering requires \mathbf{d}_E and \mathbf{d}'_E to be closer to each other (Fig. 2 right).

3.3 Assumptions on OST-HMD Setups

We use several assumptions in our calibration. In this work, we use a user-perspective camera instead of an actual human subject. Thus this work focuses more to understand the mechanism of OST-HMDs in the context of the color reproduction problem. We also use a single camera for both the world camera and the eye camera and let the camera see the world behind OST-HMDs to ignore the material distortion $m_w(\lambda)$. Thus, we assume $\mathbf{d}_c = \mathbf{d}'_E$.

Given that we use an industrial camera with calibrated gamma, we assume that the user-perspective camera has a linear camera gamma value as a diagonal matrix $\mathbf{D}_E \in \mathbb{R}_{\geq 0}^{3 \times 3}$ instead of \mathbf{g}_E . Now Eq. (8) and (7) are written as

$$\mathbf{d}_E = \mathbf{D}_E \mathbf{M} \mathbf{g}_H^{-1}(\mathbf{d}_c) + \mathbf{c}, \quad (11)$$

$$\mathbf{d}_c = \mathbf{g}_H(\mathbf{M}^{-1} \mathbf{D}_E^{-1}(\mathbf{d}_E - \mathbf{c})). \quad (12)$$

We also added a 3D constant vector $\mathbf{c} \in \mathbb{R}_{\geq 0}^3$ to the projected color. Because a display image source produces light even when the input color is completely black – i.e., the black offset [19]. Since the non-linearity of the model is represented by \mathbf{g}_H^{-1} , our calibration strategy is to first remove this non-linearity by learning non-linear, gamma correction functions, then to learn an affine transformation between the target and linearized input colors.

3.4 Semi-Parametric Color Calibration

We are now ready to explain our calibration method. For the sake of easier understanding, we will show some real measurements taken from an OST-HMD setup introduced later in the experiment section.

To be able to reproduce colors of arbitrary input colors, we require a display-dependent calibration procedure. Our calibration method uses regression to compute the parameters of a non-linear gamma response function of the display for each color channel as a pre-processing step. We then use linear regression to find parameters of user-perspective camera distortion.

First, we learn the color response of an OST-HMD by displaying synthesized images showing one synthetic color while ambient light

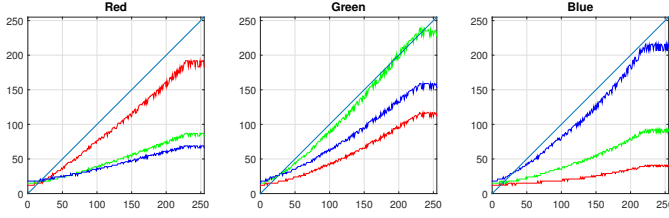


Fig. 3. Channel-wise responses of a Moverio BT-100 OST-HMD when each color channel is separately displayed. The x axes correspond to the intensity of each pure color \mathbf{d}_c and each y axis is observed color \mathbf{d}_E by a camera. Each color channel suffers from non-linear color distortions. At $x = 0$, one can see the black offsets. Note that we exclude the saturated y values in around $x > 220$ from our calibration.

is blocked, and then by capturing the displayed color with a camera. The proposed method uses channel-wise response information instead of checking all possible color combinations. We display 256 colors of each channel on the OST-HMD from black to pure colors. We then obtain three channel-wise look-up tables:

$$\{ {}^K \text{LUT}(d_K) : \mathbb{N}_{[0,255]} \rightarrow \mathbb{N}_{[0,255]} \}_K, \quad (13)$$

for each primary color $K \in \{R, G, B\}$.

Fig. 3 shows an example of the channel-wise response plots from a Moverio BT-100, a consumer OST-HMD, measured with an industrial camera. As we can see, the camera sensor has values in all channels even though the OST-HMD displayed only pure colors separately in each channel (*channel mixture problem*). This is due to different color spectra of the sensor and light source of the display. Furthermore, color transformations here are not strictly linear and the distortion brings unwanted colors into the image (*gamma problem*). Finally, note the small offset for purely black input signals (*non-black display problem*).

We will now show how each of these three problems can be reduced.

Gamma model: To correct the non-linear color distortion due to gamma, we first regress a function on the color response curve of each primary color $K \in \{R, G, B\}$. We use a 2-term power function ${}^K f(d_K | {}^K \alpha, {}^K \beta, {}^K \gamma) = {}^K \alpha + {}^K \beta * \text{pow}(d_K, {}^K \gamma)$ for this regression,

$$\{ {}^K \text{LUT}(d_K) \approx {}^K f(d_K) : \mathbb{R}_{\geq 0} \rightarrow \mathbb{R}_{\geq 0} \}_K, \quad (14)$$

as it provides reasonable approximation without performance hit. Given an input digital color $\mathbf{d} := [d_R, d_B, d_G]^T$, we treat the non-linear brightness response of the display as

$$\mathbf{g}_H^{-1}(\mathbf{d}) \approx f(\mathbf{d}) = [{}^R f(d_R), {}^B f(d_B), {}^G f(d_G)]^T, \quad (15)$$

where $f : \mathbb{R}_{\geq 0}^3 \rightarrow \mathbb{R}_{\geq 0}^3$ couples the three regressed functions. We obtain raw, linearized color response curves by plotting sets

$${}^L S_K := \{ ({}^K f(d_L), {}^K \text{LUT}(d_L)) \}, d_L \in [0, \dots, 255], \quad (16)$$

for all color channel pairs of the primary color K and subcolor L . Fig. 4 shows total 9 curves on the BT-100 setting based on each ${}^L S_K$.

Channel Mixture Model with the Black Offset: The resulting color plots are subject to linear regression on the next step.

We note the linear regression functions for each ${}^L S_K$ as

$${}^L a_K {}^L d_K + {}^L b_K = 0. \quad (17)$$

From Eq. (17), we construct linear correction transformation expressed by a 3-by-3 matrix $\mathbf{M}^{-1} \mathbf{D}_E^{-1}$ and a 3-vector \mathbf{c} :

$$\mathbf{M}^{-1} \mathbf{D}_E^{-1} \approx \underbrace{\begin{bmatrix} {}^R a_R & {}^R a_G & {}^R a_B \\ {}^G a_R & {}^G a_G & {}^G a_B \\ {}^B a_R & {}^B a_G & {}^B a_B \end{bmatrix}}_{=: \mathbf{A}}, \mathbf{c} = \begin{bmatrix} {}^R b_R + {}^G b_R + {}^B b_R \\ {}^R b_G + {}^G b_G + {}^B b_G \\ {}^R b_B + {}^G b_B + {}^B b_B \end{bmatrix} / 3 \quad (18)$$

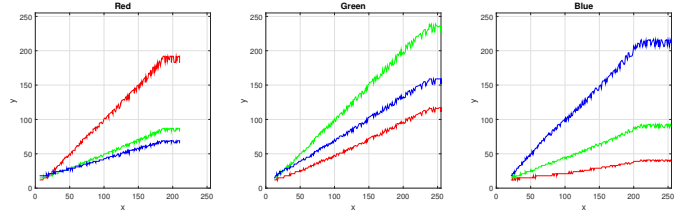


Fig. 4. Linearized channel-wise color responses of the OST-HMD based on ${}^L S_K$ from Eq. (16). In each figure, the x axis is the primary color value of the input color (e.g., $[{}^R f(d_R), 0, 0]^T$), and the y axis is the corresponding response color (e.g., $[{}^R \text{LUT}(d_R), 0, 0]^T$). In each color channel, the two subcolors are also linearized well by the channel-wise gamma correction in addition to the primary colors.

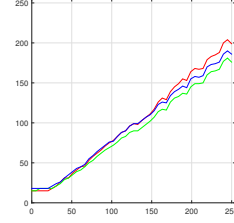


Fig. 5. Result of pre-corrected gray colors without post-scaling on EPSON BT-100. A consistent, linear scaling remains which does not coincide well with our color distortion model.

We are now ready to pre-distort a target color.

Given a target color \mathbf{d}_E , we first apply the linear correction to obtain an intermediate color vector $\tilde{\mathbf{d}}_E$:

$$\tilde{\mathbf{d}}_E := \mathbf{A}(\mathbf{d}_E - \mathbf{c}) \approx \mathbf{M}^{-1} \mathbf{D}_E^{-1}(\mathbf{d}_E - \mathbf{c}). \quad (19)$$

The target input color \mathbf{d}_c is given by simply applying inverse of the non-linear distortion to each channel:

$$\mathbf{d}_c = f^{-1}(\tilde{\mathbf{d}}_E) = f^{-1}(\mathbf{A}(\mathbf{d}_E - \mathbf{c})) \approx \mathbf{g}_H(\mathbf{d}_E). \quad (20)$$

Intensity Scaling Heuristics We observe that displaying gray-scale colors with the right-hand side of Eq. (20) on a real OST-HMD still creates an offset as shown in Fig. 5. As a heuristic, we correct this error by applying the post-scale factors to \mathbf{d}_c . To find the vector, we apply Eq. (19) and Eq. (20) to a sequence of gray-scale colors, $\hat{\mathbf{d}}_E := [d, d, d]^T$, where $d = [0 : 255]$ and measure the received colors $\hat{\mathbf{d}}_E' := [d'_R, d'_B, d'_G]^T$.

For each color channel, we find scaling parameters ${}^K s$ so that $d'_K \approx {}^K s d$, then our final target input is

$$\mathbf{d}_c = f^{-1}(\mathbf{S}^{-1} \mathbf{A}(\mathbf{d}_E - \mathbf{c})), \quad (21)$$

instead of Eq. (20). Here \mathbf{S} is $\text{diag}([{}^R s, {}^G s, {}^B s])$. We conjecture the reason is due to remaining non-linearity in the subcolors of each color after the channel-wise gamma correction.

4 TECHNICAL SETUP

We use two OST-HMD setups. In both cases, a single camera was used as a user-perspective camera.

The first setup (Fig. 6 top) uses a professional OST-HMD. We use an nVisor ST60 from NVIS. The HMD yields 1280×1024 resolution and 60° (diagonal)/ 40° (vertical) FoV, and has two DVI inputs for a right-eye and a left-eye display. Our setup uses only the left-eye display. The HMD employs LCOS (Liquid Crystal on Silicon) technology, a microdisplay technology, with a one-panel design; a single LCOS panel projects each RGB color in succession with high frequency. A semi-transparent, cubic prism in front of a user's eye reflects these light rays to the eye.

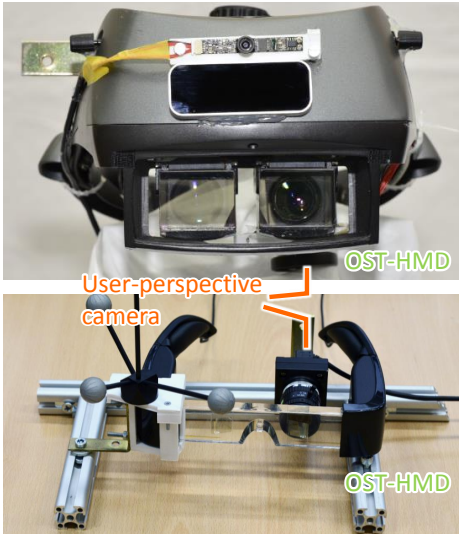


Fig. 6. Our hardware setups with (Top) a professional OST-HMD and (Bottom) a consumer OST-HMD. Components on the HMDs without annotations are not used in this paper.

The second setup (Fig. 6 bottom) uses a consumer OST-HMD. We use an MOVERIO BT-100 from EPSON. The HMD yields 960×540 resolution and 23° diagonal FoV. The left-eye display is used for the current setup. The HMD employs an HTPS TFT LCD panel with a color filter for each display. Light from the panel is guided to semi-transparent, half mirrors in front of user’s eyes, and the mirrors reflect the light to the eyes. This HMD has a composite video input. We use a VGA-composite converter (Ligawo PC-TV). It generates a composite video signal from an input digital image with 656×496 resolution. As a result, the HMD renders a stretched image compared to the original resolution.

As a user-perspective camera, we use a UI-1240ML-C-HQ from iDS together with an 8mm C-mount lens (M0814-MP2 from CBC). The camera uses a $1/1.8''$ CMOS sensor (EV76C560ACT from e2v) which provides 1280×1024 pixel images.

For experiments with a real scene, we use a physical X-Rite ColorChecker® Classic color chart which has a 4-by-6 color matrix as reference colors.

5 EXPERIMENT

We explain our calibration and our evaluation procedure in Sec. 5.1. In Sec. 5.2 and 5.3, we show the experiment results of a synthesized and a real-scene dataset done through these procedures.

5.1 Calibration and Evaluation Workflows

We first elaborate our calibration procedure conducted with the hardware listed in Sec. 4. For the user-perspective camera of each hardware setup, we set a default camera gamma value and a default white balance value. Since the nVisor ST60 OST-HMD illuminates each color channel sequentially, we also set the camera exposure time to about 1/30 second to avoid a color-breakup effect.

We calibrated the two OST-HMD setups by the following:

1. Set a user-perspective camera behind the screen of an OST-HMD and block the environment light. To block the light, we covered the entire setup with a black cloth and turned off the room light in an indoor office. For the rest of this procedure, we did not touch the setup.
2. For each of the three color channels (R,G,B), display a separate image at each intensity level $(0, \dots, 255)$, i.e. $256 \times 3 = 768$ images in all, and let the camera capture each of these to construct three LUTs: $\{^k \text{LUT}(d_k)\}_K$.

3. Compute the semi-parametric model $(A, c, f^{-1}(\cdot))$ from the collected dataset.
4. Pre-process gray-scale images by applying the above model, display the result images on the OST-HMD, and let the camera capture the rendered images. Then compute the scale factor S .

At the Step 2, since the FoV of the camera was larger than the HMD screen, we manually cropped the images so that they contain the screen area only. We took the median of each image to compute the look-up table at the step.

Our evaluation tests how calibration methods reduce the color distortion of displayed images by pre-processing the input images:

1. Input a target image I_C to an OST-HMD and capture the display screen for an output image I_E by a user-perspective camera.
2. Measure the difference between the two images in the Lab color space. We denote the image distance by $d_{\text{Lab}}(I_C, I_E)$.
3. Generate a pre-processed input image I'_C by applying the learned model to I_C .
4. Input the pre-processed image I'_C and record a corrected output image I'_E . Then compute their difference $d_{\text{Lab}}(I'_C, I'_E)$.
5. We analyze $d_{\text{Lab}}(I_C, I_E)$ and $d_{\text{Lab}}(I'_C, I'_E)$.

Ideally, we have to know corresponding pixels of two images to compute their difference by $d_{\text{Lab}}(\cdot, \cdot)$. In the following experiment sections, we elaborate how we treated this matching issue.

We performed our calibration in MATLAB® R2014b in Windows 7 OS with the Curve Fitting Toolbox 3.5 for regression analysis and the Image Acquisition Toolbox 4.8 for automated image acquisition.

5.2 Experiment with Synthetic Color Data

We evaluated our calibration method for Path A in Fig. 2 with synthetic images. Each image has a single RGB color corresponding to each of the 24 colors defined in the Macbeth Color Chart. We used the professional OST-HMD setup for the evaluation. Figure 7a top left shows all 24 target images $\{I_C\}$, arranged as a single picture. Using the synthetic data with a standard color set helps us to analyze calibration results.

Since the display screen does not fill the entire region of the output images (I_E, I'_E) , we manually cropped the images such that we could eliminate image regions that did not capture the screen. We used the median value of each image region for computing $d_{\text{Lab}}(I_C, I_E)$ and $d_{\text{Lab}}(I'_C, I'_E)$ which is a reasonable approximation of comparing each corresponding pixel independently since we only display a color per target image.

5.2.1 Baseline Method

For comparison, we implemented a baseline method adapted from the binned profile method [23, 10]. The original method is basically an LUT-based method – it builds an LUT of target and displayed colors, then applies a binary color search given a new image at the runtime. On the other hand, the baseline method searches desirable input colors without building an LUT. The method uses the user-perspective camera to measure a currently displayed color to update the input color dynamically.

The original method divides the CIE Lab color space into cubic bins with the length 2.3, which is equivalent to one Just Noticeable Distance (JND) of the human color perception. The method then collects a corresponding displayed color for each representative color in the bins to create an LUT. At the online rendering step, the method traverses the LUT to determine desirable input colors for given target colors. To reduce the traversing time, the method employs a binary search in the CIE Lab space. The data collection for all binned colors takes time. For example, their setup has to capture 8376 colors per display. Since our synthetic-data evaluation considers the 24 colors only, we decided to avoid measuring the all color combinations.

Algorithm 1 A baseline color-search method for the calibration comparison described in Sec. 5.2.1.

```

input : a target color in CIE Lab  $\mathbf{d}_0$ 
output: a pre-processed color in CIE Lab  $\mathbf{d}_{\min}$ 
1  $\mathbf{d}_{\min} \leftarrow \mathbf{d}_0$ 
2  $s \leftarrow 30, s_{\min} \leftarrow 2.5$  // Initial/Minimum search range
3  $D \leftarrow \{[a, b, c]^T\}$  for  $\forall a, b, c \in \{-1, 0, 1\}$ 
4 while  $s > s_{\min}$  do
5    $\Delta \mathbf{d}_{\text{best}} = [0, 0, 0]^T$ 
6   // Evaluate neighborhood colors
7   foreach  $\Delta \mathbf{d} \in D$  do
8      $\mathbf{d} \leftarrow \mathbf{d}_{\min} + s\Delta \mathbf{d}$ 
9     Display  $\mathbf{d}$  on an OST-HMD
10    Measure the output  $\mathbf{d}'$  by a user-perspective camera
11    if  $d_{\text{Lab}}(\mathbf{d}, \mathbf{d}') < d_{\min}$  then
12       $\Delta \mathbf{d}_{\text{best}} \leftarrow \Delta \mathbf{d}$  // Best neigh. direction
13     $\mathbf{d}_{\min} \leftarrow \mathbf{d}_{\min} + s\Delta \mathbf{d}_{\text{best}}$ 
14     $s \leftarrow s/1.5$  // Decrease the search range

```

Our baseline method is based on a dynamic binary search without constructing an LUT – it dynamically updates an input color based on the measured color difference between the target color and the current output. The update employs the binary search strategy from the original method, thus the search will find a color within a *color bin* which has the specified search range.

Algorithm 1 shows the detail of our baseline method. Given a target color, the algorithm searches the best input color by recursively testing colors that are distant at given search range of the current input. A scalar value s_{\min} determines the search range in the CIE Lab color space, i.e. it is equivalent to use the original binned profile method with the unit cube of size s_{\min} . Through the experiment sections, we assume that the CIE Lab color space is in the range of $L \in [0, 100]$, $a, b \in [-127, 127]$. Note that we search 26 ($= 3^3 - 1$) neighborhood colors instead of 6 in the original method. We also tested the baseline method with the minimum search range $s_{\min} = 0.5$. This setting is roughly equivalent to set the bin size to length 1 in the CIE Lab space, thus provide ideally best Lab color found among integer Lab colors.

Note that we used our baseline method for the synthetic evaluation only since it is designed for calibrating one color per image without the need of handling the spatial registration between input and output images.

5.2.2 Experiment Results

Figure 7 summarizes the evaluation results. As Fig. 7a top right shows, original output images $\{\mathbf{I}_E\}$ have color distortion. A chromaticity plot out of all the images shows that the distortion shrinks the input colors. Fig. 7a left column shows the original and pre-processed images that were sent to the display. The proposed method created 11 pre-processed colors that have values higher than 255 and/or lower than 0. We had to crop these colors so that they are kept in the display color range. One can see from Fig. 7a right column that all three corrected output images regain the target colors compared to the output by the original image (Fig. 7a top right).

Figure 7b left shows measured color differences of each input color. By our method, 18 of 24 images regained color closer to the target. On the other hand, the baseline method achieved the best result for each color. This is expected since the method searches the closest color among the possible color combinations. However, as we explained in the related work, the original binned profile method needs an intensive data collection to construct an LUT and requires to run a binary search per pixel at runtime. In the baseline method, setting the minimum search range s_{\min} to 0.5 did not change the result much, which supports that the choice of bin size 2.3 in [23, 10] is sufficient for the LUT size without huge accuracy loss.

Figure 7b right shows the Receiver Operating Characteristic (ROC)

curve of the measured color differences. The baseline methods have 13 colors that are less than 1 JND ($x=2.3$). When color difference is roughly $x>20$, ours and the baseline method perform almost equivalently.

In some input colors, none of the methods could achieve low color differences compared to other colors. Since all methods failed in these input colors, it is likely that the color gamut of the display was not large enough to reproduce those target colors.

5.3 Experiment with Real Image Data

We evaluated the proposed method by using a real-scene image taken by a camera. The purpose of using a real-scene image is to see the capability of the method for AR applications that possibly require to display visually processed images taken from scene cameras.

Before conducting the calibration procedure in each OST-HMD setup, we let the user-perspective camera captures the color checker board as a target image, i.e. we treated the camera as a world camera. The camera captured the board through the semitransparent medium of each HMD. Unlike the previous experiment, input and output images contain 24 color cells at once. We thus rectified the images in the evaluation (see images in Fig. 8a), and we manually took the ROI of each color cell in the rectified images to compute color difference for each color separately.

Figure 8 and 9 summarize the evaluation result of the two OST-HMD setups respectively. Color distortion characteristics are different in the two setups. The professional OST-HMD tends to loose green color (Fig. 8a top right) while the consumer OST-HMD shifts the input colors to the blue direction. In both setups, calibration results improved the color reproduction quality (Fig. 8 and 9).

6 DISCUSSION

We discuss limitations in the current calibration method and hardware for practical OST-HMD color calibrations in future AR applications.

6.1 Eye Model Issues

Although we did not test our method with human subjects, we should consider the following eye-related calibration issues.

Sensitivity Estimation of User’s Eyes Our experiment setup treated the eye as a camera and replaced with user-perspective cameras for the evaluations. In practice, the eye does not have the same chromatic responses as cameras. Furthermore, it is hard to obtain the actual image that a user perceives. A possible solution might be to employ the corneal imaging technique which estimates a user’s view from the light reflected on the eye surface [29]. However, this technique give us information about neither how our retina absorbs incoming light nor how our brain perceives the color.

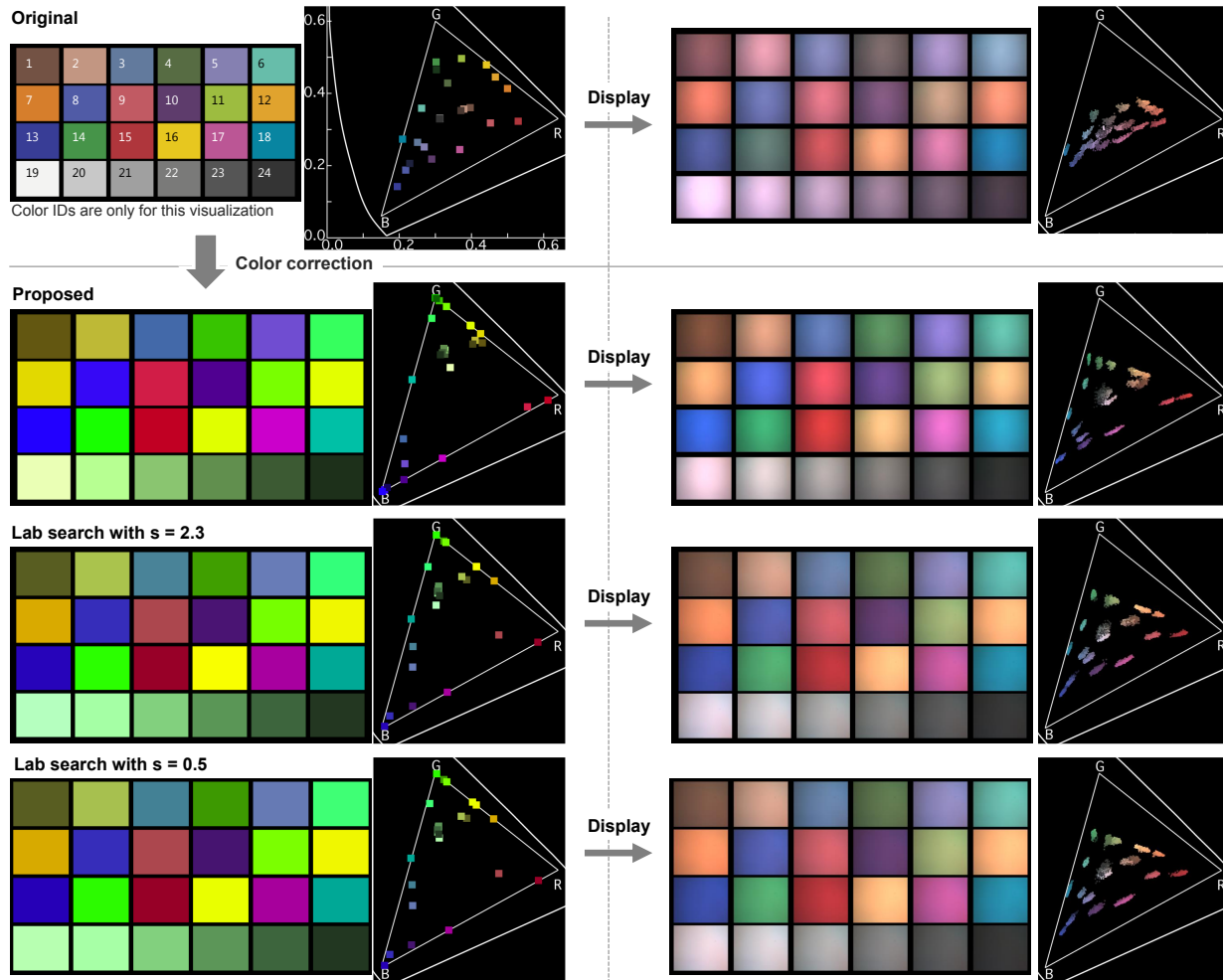
Viewpoint Estimation of User’s Eyes Similar to the above issue, the misalignment of the viewpoint between an eye and a world camera causes a problem: if we have to determine a target color by using the camera as a reference of the scene color, the misalignment possibly changes the appearance of an anisotropic surface. Aligning optical axes of the eye and the camera by a half mirror optics is a solution.

The viewpoint also affects the display color due to the imperfection of the optics of current OST-HMDs. This is analogous to PCSs with dynamic 3D scenes where a projector has to update a projected image whenever a scene object moves and the change the reflectance of the surface on which the projector casts the image.

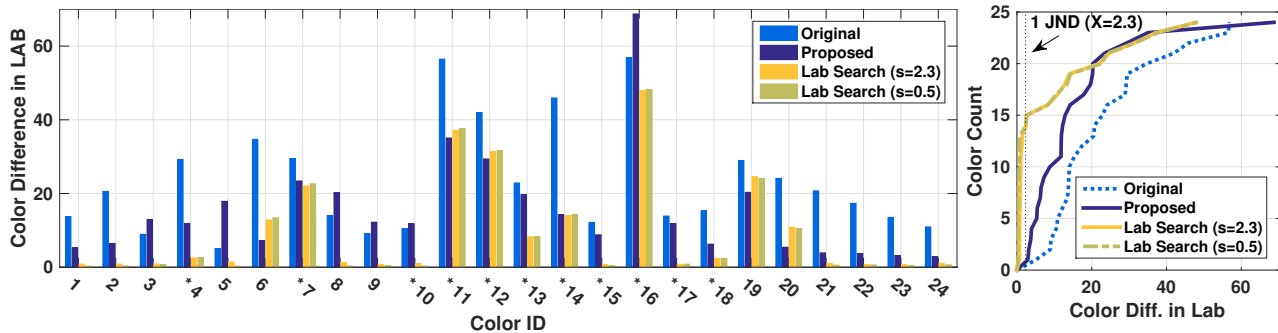
Adaptive Eye Model An eye constantly changes its pupil size. The change would affect perceived colors even if we know the radiometric response of the retina of the eye. By tracking the radius of pupils, one might be able to estimate the sensed brightness of eyes and modify color calibration parameters accordingly in real time.

6.2 HMD Model Issues

The limited capability of the current OST-HMD technology causes other issues.



(a) Images captured by the user-perspective camera and their chromaticity diagrams. We tiled 24 color images in one picture for visualization purpose in the input/output images shown above. The chromaticity diagram on the left column also have bigger color points for the same purpose. Numbers on the top left image are annotations added only for this figure.



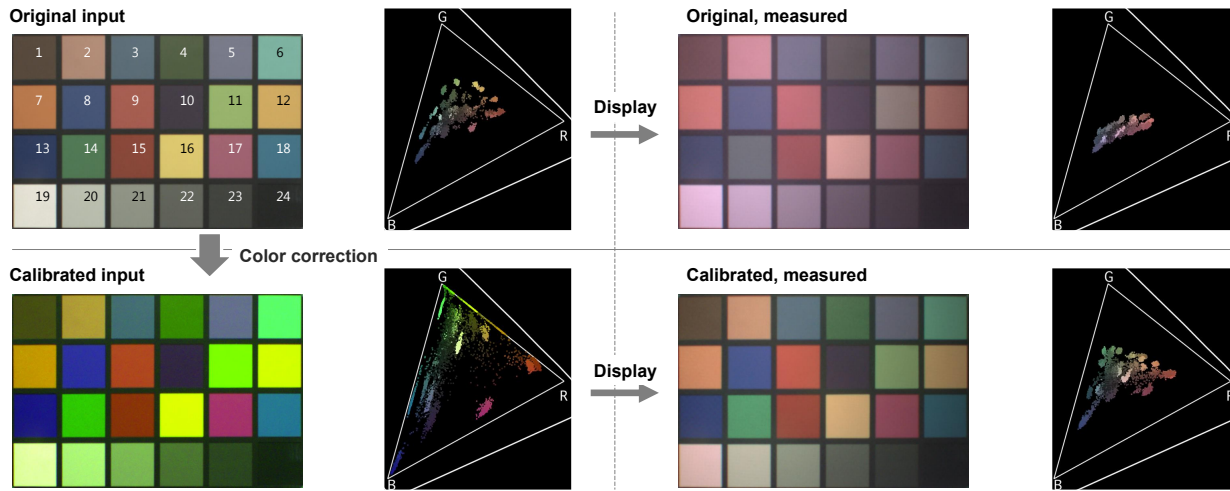
(b) (Left) Color difference of displayed images with/without the calibration methods. In color IDs, * represents the pre-processed color exceeded the range of $[0,255]$. *Lab Search* ($s=X$) are our baseline methods with the minimum search range X . Even with those ideal color search results, some color IDs have large errors. This implies that the color range of the OST-HMD was not enough to reproduce certain colors. (Right) An ROC curve of the left plot. The y axis shows the number of colors that have errors smaller than x-axis values.

Fig. 7. Evaluation of Path A in Fig. 2: Color correction results of the NVIS nVisor ST60 with the synthetic, digital color set.

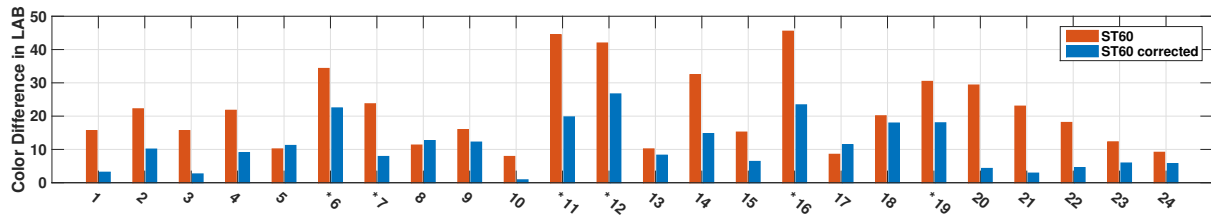
Display Color Range If the color range of an OST-HMD is extremely smaller than target colors, there is no hope for good color calibration. As we explained in the experiment section, a pre-processed color can be those out of the color range of a display. For example, when a pre-processed color contains negative values, we have to truncate the values to zero or at least to positive. Thus the displayed color would appear brighter than the target color. A workaround is to add an opaque layer to OST-HMDs to reduce the amount of light coming

into eye [5, 6]. Especially, [6] has a capability to control opaqueness by modulating its opaque LCD layers. Another solution is to find a closer target color which can be represented by a given color range of the display.

Display Color Characteristics As we saw in the experiment, most OST-HMDs have the black offsets. Since different optics have different illumination characteristics [30], we would need a modeling



(a) Input/output images and their chromaticity plot. The world camera captured the physical color chart. We used our proposed method to create the calibrated input. Numbers on the top left image are annotations only added in this figure.



(b) Color difference of displayed images with/without the calibration methods. X axis is the color ID. In color IDs, * represents the pre-processed color exceeded the range of [0,255].

Fig. 8. Evaluation of Fig. 2 right: color correction result of our method on the NVIS nVisor ST60 for the physical color chart.

of the offset for different display types. For example, nVisor ST60 has the color breaking problem due to its 3-panel LCOS projector, and the breaking might affect the offset. Moverio BT-100 uses an LCD panel with a color filter, thus the offset might be stable. If we use retinal scanning OST-HMDs that uses lasers, then theoretically they do not have the black offset.

Distortion by Optical Media of OST-HMDs The optical media of OST-HMDs interfere light from both the display light source and the scene [23]. Although these are not as critical as the display characteristics, we observed in our OST-HMDs that such elements dim the environment light. This would cause additional distortion between an image by world camera and an image seen by a user.

A hardware solution is to use pupil-division optical systems (e.g., Olympus MEG4.0). Their optical combiners are smaller than relative pupils size, which enables users to see the environment directly while seeing images. Therefore, we can almost ignore a part of the material distortion with these displays.

6.3 Other Issues

Error Measurements: For a formal user study, we should incorporate a subjective study design from the field of human visual perception.

World Camera Sensor: Since a world camera itself has its own sensor, it would be necessary to estimate the color response of an image sensor to further break down the OST-HMD color model.

7 CONCLUSION AND FUTURE WORK

This paper investigates a color reproduction problem of OST-HMDs for AR applications. We first formulate the problem in a similar manner to projector camera systems by considering rendering process of a general HMD-eye system. We then propose a semi-parametric color calibration method which incorporates the optical properties of the system. We evaluate our method against a baseline method which is based on a color look-up table search method. We further demonstrate our method with a real scene image. More importantly, we provide a

thorough analysis of the current limitation of our method and the color reproduction in OST-HMDs. We then discuss how to realize more practical color reproduction methods for future HMD-eye system.

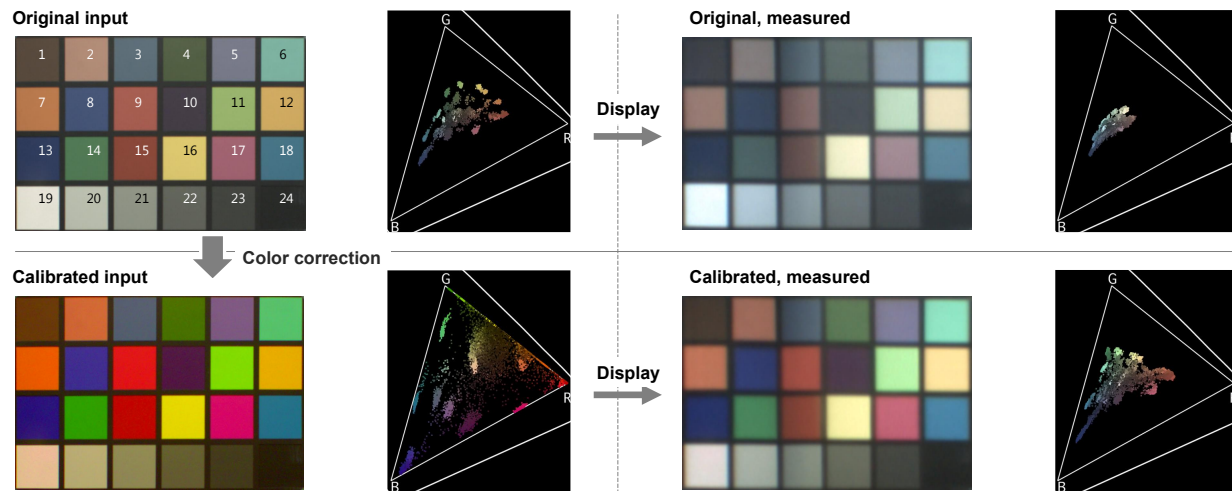
Future research direction involves: enhancing the color model to incorporate eye models or display material models, conducting user-oriented study for performance evaluations, and investigating hardware solutions such as adaptive opaque displays.

8 ACKNOWLEDGMENTS

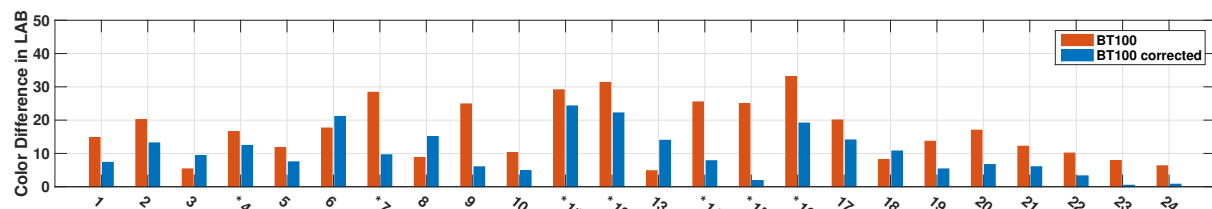
The project received funding from the European Union's Seventh Framework Programmes for Research and Technological Development under PITN-GA-2012- 316919-EDUSAFE.

REFERENCES

- [1] P. Debevec, "Rendering synthetic objects into real scenes: Bridging traditional and image-based graphics with global illumination and high dynamic range photography," in *ACM SIGGRAPH 2008 classes*. ACM, 2008, pp. 32:1–32:10.
- [2] T. Amano and H. Kato, "Appearance control by projector camera feedback for visually impaired," in *Proc. CVPRW*. IEEE, 2010, pp. 57–63.
- [3] D. G. Aliaga, A. J. Law, and Y. H. Yeung, "A virtual restoration stage for real-world objects," in *ACM Transactions on Graphics (TOG)*, vol. 27, no. 5. ACM, 2008, pp. 149:1–149:10.
- [4] Y. Itoh and G. Klinker, "Vision Enhancement: Defocus Correction via Optical See-Through Head-Mounted Displays," in *6th Augmented Human International Conference, AH '15, Singapore, March 9-11, 2015*, 2015, pp. 1–8.
- [5] K. Kiyokawa, Y. Kurata, and H. Ohno, "An optical see-through display for mutual occlusion of real and virtual environments," in *Proceedings on IEEE and ACM International Symposium on Augmented Reality (ISAR)*. IEEE, 2000, pp. 60–67.
- [6] A. Maimone and H. Fuchs, "Computational augmented reality eye-glasses," in *Proc. ISMAR*. IEEE, 2013, pp. 29–38.
- [7] C. Weiland, A.-K. Braun, and W. Heiden, "Colorimetric and photometric compensation for optical see-through displays," in *Universal Access*



(a) Input/output images and their chromaticity plot. The world camera captured the physical color chart. We used our proposed method to create the calibrated input. Numbers on the top left image are annotations only added in this figure.



(b) Color difference of displayed images with/without the calibration methods. X axis is the color ID. In color IDs, * represents the pre-processed color exceeded the range of [0,255].

Fig. 9. Evaluation of Fig. 2 right: color correction result of our method on the EPSON Moverio BT100 for the physical color chart.

- in *Human-Computer Interaction. Intelligent and Ubiquitous Interaction Environments*. Springer, 2009, pp. 603–612.
- [8] O. Cakmakci and J. Rolland, “Head-worn displays: a review,” *Journal of Display Technology*, vol. 2, no. 3, pp. 199–216, 2006.
- [9] J. P. Rolland and H. Fuchs, “Optical versus video see-through head-mounted displays in medical visualization,” *Presence: Teleoperators and Virtual Environments*, vol. 9, no. 3, pp. 287–309, 2000.
- [10] S. K. Sridharan, J. D. Hincapié-Ramos, D. R. Flatla, and P. Irani, “Color correction for optical see-through displays using display color profiles,” in *Proceedings of the 19th ACM Symposium on Virtual Reality Software and Technology*. ACM, 2013, pp. 231–240.
- [11] W. Lee and W. Woo, “Real-time color correction for marker-based augmented reality applications,” in *International Workshop on Ubiquitous Virtual Reality*, 2009, pp. 32–25.
- [12] S. B. Knorr and D. Kurz, “Real-time illumination estimation from faces for coherent rendering,” in *Proc. ISMAR*. IEEE, 2014, pp. 113–122.
- [13] J. Fischer, D. Bartz, and W. Straßer, “Enhanced visual realism by incorporating camera image effects,” in *Proc. ISMAR*. IEEE Computer Society, 2006, pp. 205–208.
- [14] C. Menk and R. Koch, “Truthful color reproduction in spatial augmented reality applications,” *Visualization and Computer Graphics, IEEE Transactions on*, vol. 19, no. 2, pp. 236–248, 2013.
- [15] M. Brown, A. Majumder, and R. Yang, “Camera-based calibration techniques for seamless multiprojector displays,” *Visualization and Computer Graphics, IEEE Transactions on*, vol. 11, no. 2, pp. 193–206, 2005.
- [16] A. Ilie and G. Welch, “Ensuring color consistency across multiple cameras,” in *Proc. ICCV*, vol. 2. IEEE, 2005, pp. 1268–1275.
- [17] A. Madi and D. Ziou, “Color constancy for visual compensation of projector displayed image,” *Displays*, vol. 35, no. 1, pp. 6–17, 2014.
- [18] A. Majumder, Z. He, H. Towles, and G. Welch, “Achieving color uniformity across multi-projector displays,” in *Visualization 2000. Proceedings*. IEEE, 2000, pp. 117–124.
- [19] A. Majumder, “Properties of color variation across multi-projector displays,” *Proceedings of SID Eurodisplay*, vol. 2002, pp. 1–4, 2002.
- [20] R. D. Myers, “Method and system for color matching between digital display devices,” Jun. 6 2000, US Patent 6,072,902.
- [21] F. Porikli, “Inter-camera color calibration by correlation model function,” in *Proceedings on International Conference on Image Processing (ICIP)*, vol. 2. IEEE, 2003, pp. 133–136.
- [22] M. D. Grossberg, H. Peri, S. K. Nayar, and P. N. Belhumeur, “Making one object look like another: Controlling appearance using a projector-camera system,” vol. 1. IEEE Computer Society, 2004, pp. 452–459.
- [23] J. David Hincapié-Ramos, L. Ivanchuk, S. K. Sridharan, and P. Irani, “Smartcolor: Real-time color correction and contrast for optical see-through head-mounted displays,” in *Proc. ISMAR*. IEEE, 2014, pp. 187–194.
- [24] S. Kagarlitsky, Y. Moses, and Y. Hel-Or, “Piecewise-consistent color mappings of images acquired under various conditions,” in *Proc. ICCV*. IEEE, 2009, pp. 2311–2318.
- [25] D. Jameson and L. M. Hurvich, “Theory of brightness and color contrast in human vision,” *Vision Research*, vol. 4, no. 1, pp. 135–154, 1964.
- [26] A. Gijsenij, T. Gevers, and J. Van De Weijer, “Computational color constancy: Survey and experiments,” *Image Processing, IEEE Transactions on*, vol. 20, no. 9, pp. 2475–2489, 2011.
- [27] E. Reinhard, M. Ashikhmin, B. Gooch, and P. Shirley, “Color transfer between images,” *IEEE Computer graphics and applications*, vol. 21, no. 5, pp. 34–41, 2001.
- [28] S. K. Nayar, H. Peri, M. D. Grossberg, and P. N. Belhumeur, “A projection system with radiometric compensation for screen imperfections,” in *ICCV workshop on projector-camera systems (PROCAMS)*, vol. 3. Cite-seer, 2003.
- [29] C. Nitschke, A. Nakazawa, and H. Takemura, “Corneal Imaging Revisited: An Overview of Corneal Reflection Analysis and Applications,” *IPSP Trans. Computer Vision and Applications*, vol. 5, pp. 1–18, 2013.
- [30] P. Bodrogi and T. Q. Khanh, “Colorimetric and color appearance-based characterization of displays,” *Illumination, Color and Imaging: Evaluation and Optimization of Visual Displays*, pp. 25–95, 2012.